Size-Selective Synthesis of Mesoporous LiFePO₄/C Microspheres based on Nucleation and Growth Rate Control of Primary Particles

Min-Young Cho[a,b], Haegyeom Kim[c], Hyungsub Kim[c], Young Su Lim[a], Kwang-Bum Kim[b], Jae-Won Lee[d], Kisuk Kang[c,e]*, Kwang Chul Roh[a],*

[a] Energy Materials Center, Green Ceramics Division, Korea Institute of Ceramic Engineering & Technology, 233-5 Gasan-dong, Guemcheon-Gu, Seoul 153-801, Republic of Korea.

[b] Department of Materials Science & Engineering, Yonsei University, 50 Yonsei-ro, Seodaemun-Gu, Seoul 120-749, Republic of Korea.

[c] Department of Materials Science and Engineering, Seoul National University, 599 Gwanak-ro, Gwanak-gu, Seoul 151-741, Republic of Korea.

[d] Department of Energy Engineering, Dankook University, Cheonan 330-714, Republic of Korea.

[e] Center for Nanoparticle Research, Institute for Basic Science (IBS), Seoul National University, 1 Gwanak-ro, Gwanak-gu, Seoul 151-742, Republic of Korea.

E-mail: rkc@kicet.re.kr(Kwang Chul Roh)
E-mail: matlgen1@snu.ac.kr (Kisuk Kang)

Electronic Supplementary Information (ESI†)

CONTENTS

Table S1 Lattice parameters and unit cell volumes for LFP/C

Sample	Lattice parameter			Unit cell volume (Å^3)
	a (Å)	b (Å)	c (Å)	
C1-LFP/C	10.312991(18)	5.997994(9)	4.688861(8)	290.0401
C2-LFP/C	10.315160(18)	5.998934(10)	4.689956(8)	290.2143
C3-LFP/C	10.314023(18)	5.998675(10)	4.689209(8)	290.1235

**Table S2** Carbon contents determined by the carbon/sulfur (CS) determinator for the precursors and LFP/C

Sample	C1-LFP	C2LFP	C3LFP
Carbon (wt %)	0.06	0.11	0.08
Sample	C1-LFP/C	C2-LFP/C	C3-LFP/C
Carbon (wt %)	3.13	3.62	3.67

**Table S3.** Rietveld refinement results and antisite defect concentrations for C1-LFP/C, C2-LFP/C, and C3-LFP/C.

Sample	Atom	Site	Multiplicity	X	Y	Z	B_{iso}	Occupancy
	Li^{+1}	Li1	4	0	0	0	3.7(3)	0.97996
C1-LFP/C	Fe^{+2}	Li1	4	0	0	0	3.7(2)	0.02004
	P	P1	4	0.09568(16)	0.25000	0.4187(3)	0.94(5)	1.00000
Antisite	O^{-2}	O1	4	0.0957(4)	0.25000	0.7419(7)	0.56(10)	1.00000
defects	O^{-2}	O2	4	0.4562(4)	0.25000	0.2083(7)	0.76(9)	1.00000
2.004%	O^{-2}	O3	8	0.1655(3)	0.0462(4)	0.2850(4)	0.65(7)	1.00000
	Li^{+1}	Li1	4	0	0	0	3.1(2)	0.98008
C2-LFP/C	Fe^{+2}	Li1	4	0	0	0	3.1(2)	0.01992
	P	P1	4	0.09545(16)	0.25000	0.4182(3)	1.37(5)	1.00000
Antisite	O^{-2}	O1	4	0.0959(4)	0.25000	0.7424(8)	1.22(10)	1.00000
defects	O^{-2}	O2	4	0.4561(4)	0.25000	0.2092(7)	0.99(9)	1.00000
1.992%	O^{-2}	O3	8	0.1643(3)	0.0472(4)	0.2839(4)	1.22(7)	1.00000
	Li^{+1}	Li1	4	0	0	0	2.4(2)	0.98000
C3-LFP/C	Fe^{+2}	Li1	4	0	0	0	2.4(2)	0.02000
	P	P1	4	0.09520(17)	0.25000	0.4189(4)	1.19(5)	1.00000
Antisite	O^{-2}	O1	4	0.0939(4)	0.25000	0.7430(8)	1.06(11)	1.00000
defects	O^{-2}	O2	4	0.4562(4)	0.25000	0.2139(7)	0.60(9)	1.00000
2.000%	O^{-2}	O3	8	0.1633(3)	0.0474(5)	0.2839(5)	0.92(8)	1.00000
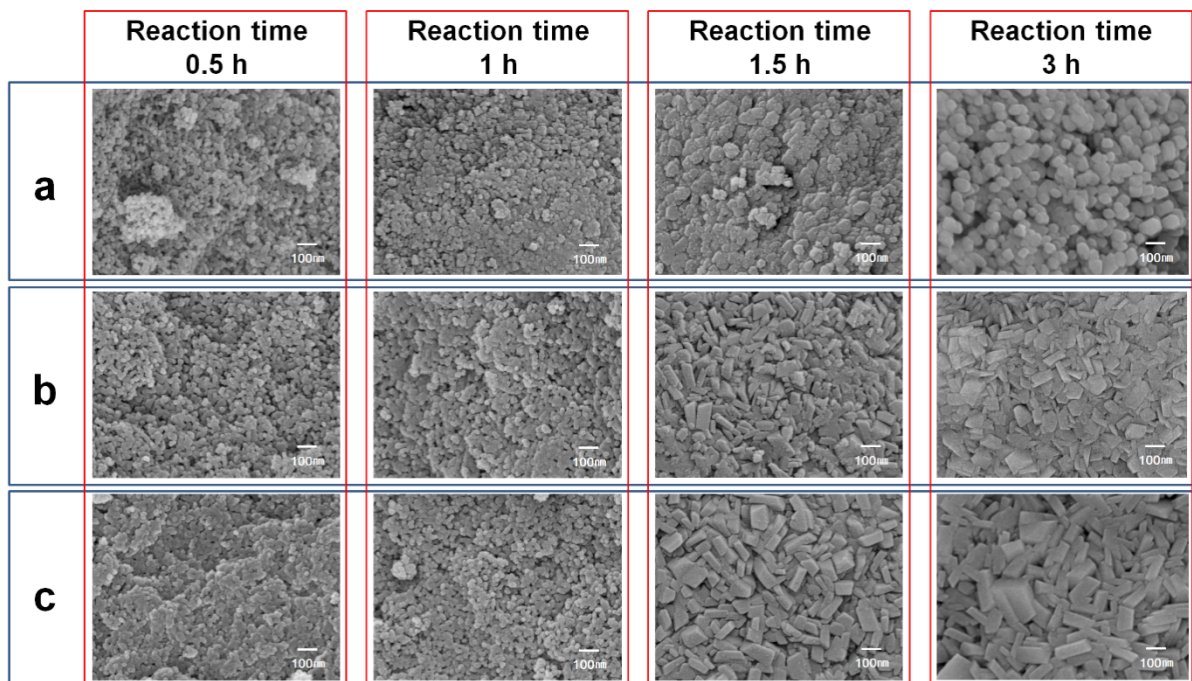
Fig. S1 Surface FE-SEM images of as-prepared precursors for different reaction times. (a) C1-LFP, (b) C2-LFP, and (c) C3-LFP. The morphologies and sizes of primary particles changed depending on the CTAB concentration.
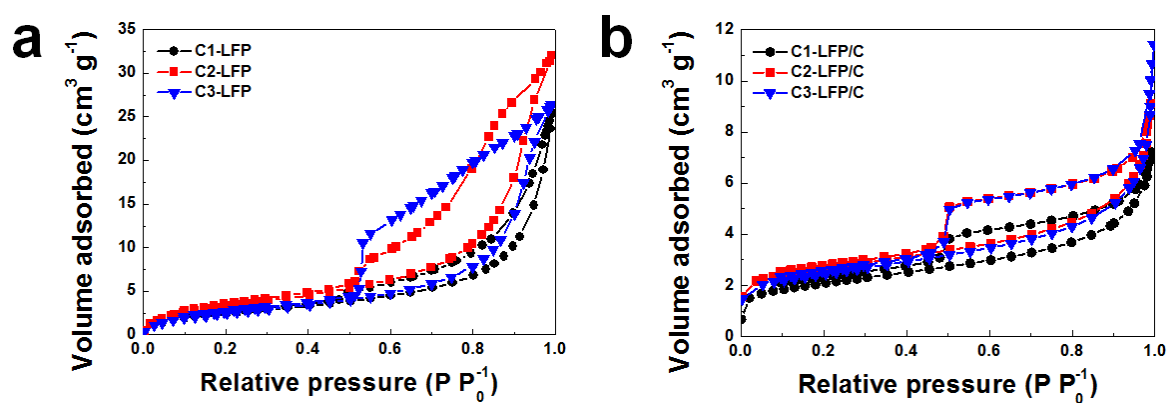
Fig. S2 Nitrogen adsorption-desorption curves. The precursors and LFP/C particles show type-IV isot herms with large type H2 hysteresis loops, indicating the mesoporous structure.
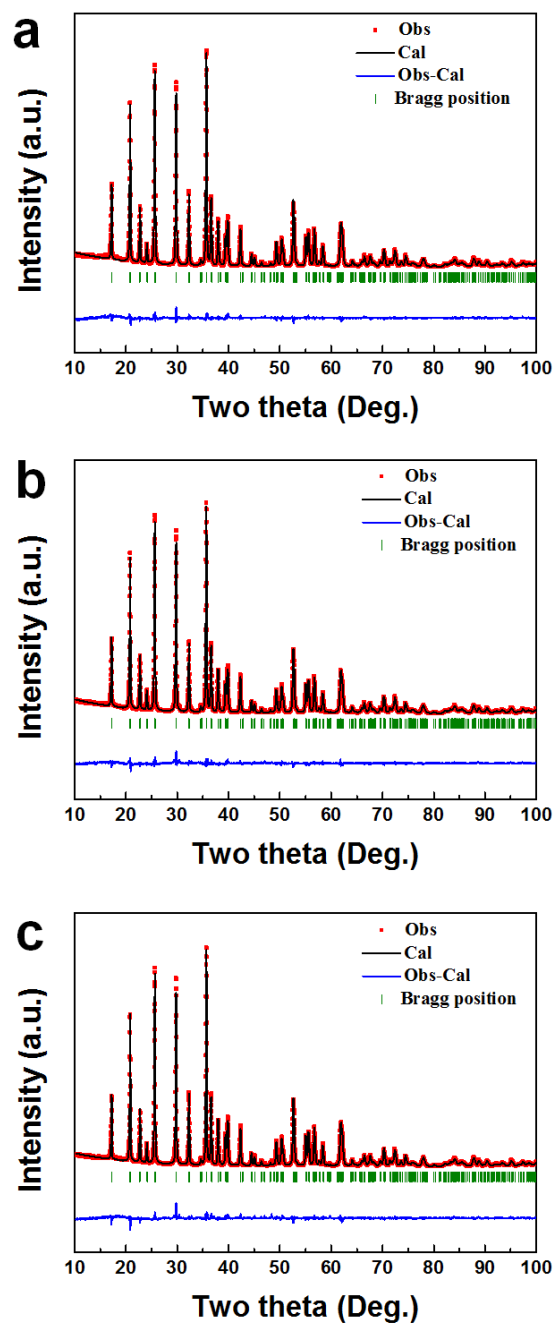
Fig. S3. Rietveld refinements of the XRD patterns for (a) C1-LFP/C, (b) C2-LFP/C, and (c) C3-LFP/C. The *R*-factors for the XRD patterns are R_p = 6.75 %, R_I = 7.86 %, R_F = 2.98 %, and S = 0.795; R_p = 5.04 %, R_I = 7.98 %, R_F = 3.40 %, and S = 0.816; and R_p = 5.73 %, R_I = 8.04 %, R_F = 4.19 %, and S = 1.01 for C1-LFP/C, C2-LFP/C, and C3-LFP/C, respectively.